

Inhibitory Effects of Decoy-ODN Targeting Activated STAT3 on Human Glioma Growth *In Vivo*

JIE SHEN, RONGHUI LI and GANG LI

Department of Neurosurgery, Qi Lu Hospital of Shandong University, Shandong Province, P.R. China

Abstract. *Background:* It has been previously found that a constitutively activated signal transducer and activator of transcription 3 (STAT3) blocked by decoy-ODN led to glioma growth inhibition *in vitro*. The objectives of this study were to identify whether STAT3 decoy-ODN had the same effect or not *in vivo*. *Materials and Methods:* Western blot was used to detect p-STAT3 in glioma and normal brain tissue. U251 cells were subcutaneously injected into nude mice and decoy-ODN was intratumorally administrated. TUNEL was used to examine the apoptosis cells in xenografts. Genes regulated by STAT3 were evaluated by RT-PCR and immunohistochemistry. *Results:* Activated STAT3 was highly present in glioma but not normal brain tissues. STAT3 decoy-ODN could significantly suppress the growth of glioma by inhibiting proliferation and promoting apoptosis in xenografts. The target genes controlled by STAT3 were down-regulated at both transcription and translation levels. *Conclusion:* The present study suggested that decoy-ODN provide an effective therapeutic approach to treat glioma *in vivo*.

Glioma is the most common primary brain tumor in the central nervous system. In the past decade, many traditional therapeutic approaches for glioma have been performed, including surgical resection, chemotherapy, radiotherapy and immunotherapy. However, there has been no obvious development in patient's survival. Novel strategies are required to significantly improve patients' conditions in this refractory disease.

Signal transducer and activator of transcription 3 (STAT3), is a transcription factor which is present in the cytoplasm, dimerizing and translating into the nucleus after being activated by tyrosine phosphorylation (1). In the nucleus, p-

STAT3 bind to special DNA elements (2) and promote downstream gene expression, such as bcl-2, bcl-x1, cyclin D1 and survivin, which regulate cell differentiation, growth, survival, proliferation and apoptosis. Studies have confirmed that many solid malignancies, such as breast, prostate, lung, pancreas, head and neck tumor, and glioma (3-8), exhibit constitutively activated STAT3. Until now, several strategies have been performed to block the signaling pathway of STAT3, including dominant negative, antisense, interference (siRNA) and double-stranded and single-stranded "decoy" oligonucleotides (3, 4, 7). The double-stranded decoy-ODN could correspond to specific DNA-response elements that regulate gene expression (8). Meanwhile, many studies have confirmed that decoy-ODN, such as NF-kB, E2F and AP-1 decoy-ODN, are highly specific and easily transfected into special tissues and/or cells (9-12). In a previous study (13), it has been reported that blockade of the STAT3 signal pathway via decoy-ODN could significantly suppress the growth of malignant glioma by down-regulating STAT3 downstream oncogenes *in vitro*. However, there was little information available about the condition *in vivo*. In this study, it was found that the level of phospho-STAT3 in glioma tissues was consistent with the malignant degree of glioma according to WHO classification when compared with normal brain tissue, and blocking activated STAT3 with decoy-ODN showed an obvious inhibitory effect on glioma growth *in vivo*. These results confirmed the probability of activated STAT3 as a potential target for glioma gene therapy with decoy-ODN *in vivo*.

Materials and Methods

Cell line and cell culture. The human GBM cell line, U251, conserved at Qi Lu Hospital, China, was cultured in DMEM medium (Gibco/BRL, Grand Island, NY, USA) supplemented with 10% fetal bovine serum (FBS) and antibiotics (200 IU/mL penicillin and 200 µg/mL streptomycin). Cells were maintained at 37°C in a 5% CO₂ environment.

Human tissue specimens and patients' information. Primary glioma tissues were obtained from 60 patients undergoing surgical resection at the Department of Neurosurgery, Shandong University Qi Lu

Correspondence to: Gang Li, MD, Ph.D., Department of Neurosurgery, Qi Lu Hospital of Shandong University, 107 Wenhua Western Road, Jinan 250012, Shandong Province, P.R. China. Tel: +86 0531 8216 9477, Fax: +86 0531 8216 9477, e-mail: doctorligang@126.com

Key Words: Glioma, STAT3, decoy-ODN, *in vivo*.

Hospital from October, 2005 to October, 2006. The information of the tissues is listed in Table I. Samples of normal brain tissue were obtained from 5 control subjects without cancer undergoing a decompression procedure. The samples were collected after informed consent was obtained from the patients at the time of surgery. Tissues were immediately snap-frozen in liquid nitrogen within 15-20 min after surgical removal.

Antibodies and reagents. Anti-STAT3, anti-phospho-specific STAT3 (Tyr705, Ser727), anti-bcl-x1, anti-bcl-2, anti-cyclin D1, anti-Ki67 and anti-β-actin antibodies and horseradish peroxidase-conjugated second antibody were purchased from Cell Signaling Technology (New England BioLabs, USA). Sense and antisense strands of STAT3 decoy or scramble-ODNs were synthesized using phosphorothioate chemistry by Expedite™ Nucleic Acid Synthesis System (Takara Biotechnology, Dalian). The STAT3 decoy-ODN sequence was 5'-CATTTCCCGTAAATC-3', 3'-GTAAAGGGCATTAG-5' and the scramble-ODN sequence was 5'-CATCTTGCCAATATC-3', 3'-GTAGAACGGTTATAG-5'. The sense and antisense strands were annealed and purified by HPLC (8, 13).

Tumor growth in xenografted mice. U251 cells (5×10⁶ per mouse) were harvested and re-suspended in 150 μL DMEM media and injected s.c. into right flank of female athymic nude mice (16) (Balb-nu/nu, 4 weeks old, weighing 17±2 g, Chinese Academy of Sciences, Shanghai). Approximately 7 days later, when the tumor nodules were monitored externally by palpation, the mice were randomly divided into three groups with six mice in each treatment group (PBS, STAT3 scramble-ODN and STAT3 decoy-ODN). Mice were intratumorally injected daily for a total of 44 days with 25 μg ODN in 50 μL PBS or 50 μL PBS. Tumor sizes were measured by length (l) and the width (w) every 4 days and the tumor volumes were calculated using the following formula: tumor volume=lw²/2. After the last injection, the mice were killed. The tumors were removed, part of which were fixed in formalin and embedded in paraffin for immunohistochemistry; and part of which were frozen for later tissue extraction. Experiments were repeated twice to ensure reproducibility. All the mice were maintained at an animal facility under pathogen-free conditions. The handling of mice and experimental procedures were conducted in accordance with experimental animal guidelines.

Semi-quantitative reverse transcription-PCR (RT-PCR) assay. To analyze the mRNA levels of STAT3 targeted genes, RT-PCR was performed as previously described (17). Briefly, tumor tissues were lysed in TRIzol (Invitrogen, Carlsbad, CA, USA) for total-RNA. Two microgram of RNA extraction was reverse transcribed using M-MLV Reverse Transcriptase (Invitrogen). For PCR, 2 μL cDNA was subsequently amplified with the corresponding gene-specific primers (13, 15) which were synthesized by Shanghai Genecore Biotechnologies (Shanghai, P.R. China). The bands were examined by densitometry using AlphaEaseFC software.

Western blotting. As described previously (15), U251 cells or tumor tissues were lysed and the protein concentrations were determined by the Bradford assay. The whole cell extracts (30 μg/lane) were separated by SDS-PAGE on 10% gel and transferred to a nitrocellulose membrane. After blocking with 5% non-fat milk in TBST, membranes were stained with anti-STAT3, anti-phospho-specific STAT3, or anti-β-actin antibody (at a dilution of 1:1000) in

Table I. *Clinical characteristic of 60 glioma patients.*

	Percentage (%)
Gender	
Male	38 (63.3%)
Female	22 (36.7%)
Age	
<20	7 (11.7)
20-39	16 (26.7)
40-59	26 (43.3)
≥60	11 (18.3)
Tumor site	
Frontal lobe	27 (45.0%)
Temporal lobe	12 (20.0%)
Parietal lobe	5 (8.3%)
Thalamus	3 (5.0%)
Lateral ventricle	4 (6.7%)
Cerebellar hemisphere	9 (15.0%)
WHO grade	
II	12 (20.0%)
III	18 (30.0%)
IV	30 (50.0%)
Tumor boundary	
Well-defined	14 (23.3%)
Poor-defined	46 (76.7%)

TBST and 1% BSA, respectively. After washing with TBST (5 min each) 3 times, the membranes were incubated with secondary antibodies conjugated with horseradish peroxidase in TBST and 1% BSA for 60 min. Subsequently, membranes were extensively washed with TBST and developed with an enhanced chemiluminescence (ECL) system (Pierce, Rockford, IL, USA) using X-ray film.

Terminal deoxynucleotidyl transferase-mediated nick end labeling assay (TUNEL). TUNEL assay was performed by using the In situ Cell Death Detection kit POD (Roche Applied Science, Germany). Briefly, after incubation with proteinase K (18 μg/mL) for 20 minutes, the slides were rinsed with PBS for 5 minutes, then blocked with fetal bovine serum for 15 minutes at room temperature. The TUNEL reaction mix was added to the slides and incubated in a humidified chamber for 60 minutes at 37°C. After rinsing with PBS, the slides were visualized and photographed by fluorescence microscopy. TUNEL-positive cells exhibit green fluorescence and are counted by Image-pro Plus 5.0 software. For each group, 3 samples were evaluated and 5 random fields of view were quantitated on each section. The number of apoptotic cells per high power field (HPF) was calculated.

Immunohistochemistry. The immunohistochemical staining was performed using peroxidase labeled streptavidin-biotin method (Histostain plus kits, ZYMED, CA, USA) according to the manufacturer's protocol. Briefly, after incubation with endogenous peroxidase by 3% H₂O₂, the slides were blocked with normal goat serum for 15 minutes in a humidified chamber at room temperature and then incubated at 4°C overnight with appropriate primary antibody (dilution 1:100). Next, these slides were treated with biotinylated secondary antibody for 15 minutes, and finally incubated with streptavidin-peroxidase conjugate (S-A/HRP) for 15 minutes.

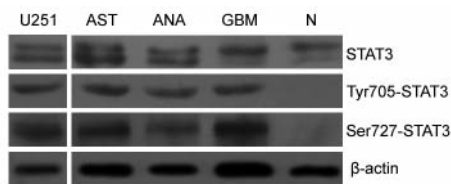


Figure 1. *STAT3* was constitutively activated in glioma tissues and U251 cells. The whole cells or tissues extracts (30 μ g/lane), prepared as in Materials and Methods, were separated by SDS-PAGE and then examined by western blotting using anti-*STAT3*, anti-phospho-specific *STAT3* (Tyr705, Ser727), or β -actin antibodies. This represents different tumor tissues. AST: diffuse astrocytoma (WHO grade II); ANA: anaplastic astrocytoma (WHO grade III); GBM: glioblastoma multiforme (WHO grade IV); N: normal brain tissue.

Immunologic reaction was developed using 3, 3-diaminobenzidine (DAB substrate kit, Boster, Wuhan). Positive cells were mounted by Image-Pro Plus5.0 software. Negative controls were performed by substituting the primary antibody with Tris-buffered saline.

Statistical analysis. All of the values were presented as the mean \pm SD for three or more individual experiments. SPSS software (version 10.0, SPSS Inc.) was used to test for significance, *p*-values <0.05 were considered statistically significant.

Results

STAT3 was constitutively activated in human glioma tissues in accordance with the malignant degree of glioma. It has been previously proved the activated *STAT3* was present in glioma tissues, however, the relationship between tumor malignant degree and activated *STAT3* was unknown. In order to identify the underlying relationship, 60 tumor specimens and U251 cell line were evaluated by Western blot with anti-*STAT3* and anti-phospho-specified *STAT3* (Tyr705, Ser727) antibodies, while five normal brain tissues were provided as control. As shown in Figure 1, *STAT3* was phosphorylated on both Tyr705 and Ser727 in tumor specimens and U251 cells. The frequency of Tyr705-*STAT3* in diffuse astrocytoma (WHO grade II), anaplastic astrocytoma (WHO grade III) and glioblastoma multiforme (WHO grade IV) was 16.7% (2/12), 88.9% (16/18) and 100% (30/30), respectively. Likewise, the frequency of Ser727-*STAT3* in the tumors above was 8.3% (1/12), 27.8% (5/18) and 100% (30/30), respectively. By contrast, activated *STAT3* in normal brain tissues was not detected. These results clearly exhibited a correlation that activated *STAT3* levels paralleled with the malignant degree of glioma according to the WHO classification.

STAT3 decoy-ODN suppressed human glioma growth *in vivo*. To determine whether *STAT3* decoy-ODN inhibits tumor growth *in vivo*, U251 cells were inoculated subcutaneously into right flanks of nude mice. On the 8th day after

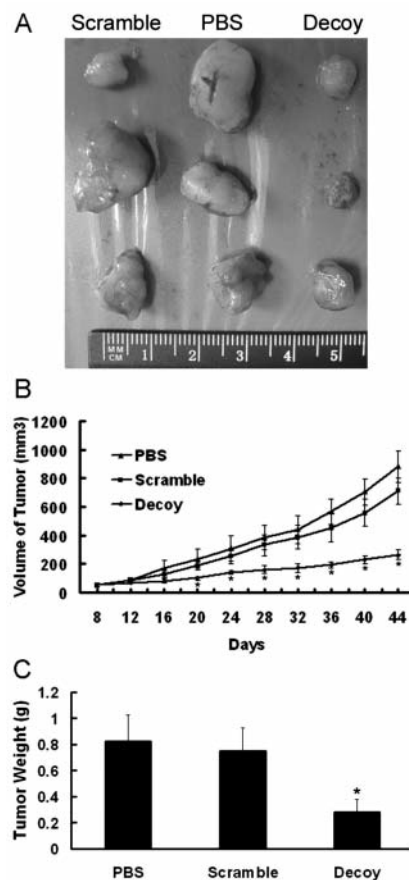


Figure 2. Blocking *STAT3* suppressed tumor growth *in vivo*. To determine growth-inhibitory effects of *STAT3* decoy-ODN *in vivo*, U251 cells (5×10^6) were inoculated subcutaneously in right flanks of nude mice. (A) Xenograft tumors harvested from each group. (B) Treatment with *STAT3* decoy-ODN led to a significant growth inhibition of tumor when compared to controls (**p*<0.05). (C) Final tumor weights in *STAT3* decoy-ODN treated group were significantly lower than that in control groups (**p*<0.05).

inoculation the tumors were established, the mice were randomly divided into three groups and treated with *STAT3* decoy-ODN, scramble-ODN or PBS, respectively. On the 44th day, the mice were sacrificed and the subcutaneous xenografts were harvested (Figure 2A). According to tumor growth curves (Figure 2B), on the 20th day after inoculation, the growth of tumors treated with *STAT3* decoy-ODN was remarkably inhibited compared with that of the control group. On the last day, the tumor volume in *STAT3* decoy-ODN treatment group was 265 ± 33 mm³, whereas the PBS control group increased to 884 ± 111 mm³, the tumor growth was inhibited by 70.0% (*p*<0.01). Further, the final average tumor weight in *STAT3* decoy-ODN treatment group was 0.28 ± 0.1 g, only 34.1% of that in the PBS control group (Figure 2C).

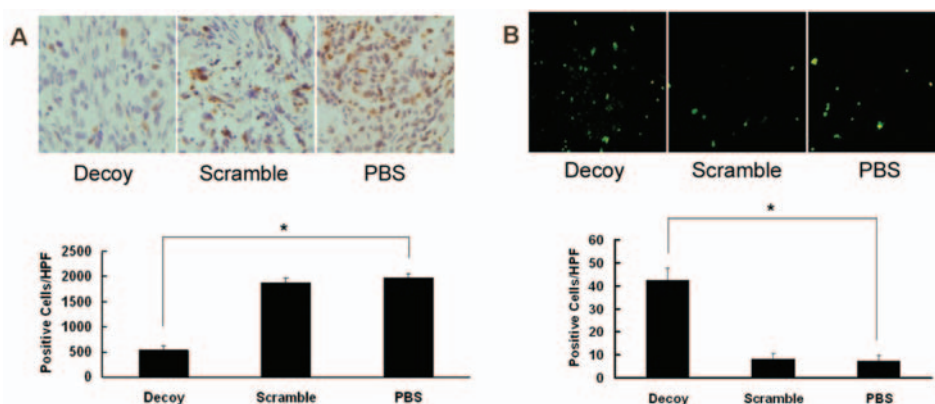


Figure 3. Blocking STAT3 inhibited proliferation and promoted apoptosis *in vivo*. (A) Immunohistochemistry of the proliferation-associated marker Ki67 in control groups or tumor xenografts treated with decoy-ODN. Quantification of the brown cells showed a statistically significant decrease in the decoy-ODN treatment group (* $p < 0.05$). (B) TUNEL assay demonstrated the apoptotic cells in STAT3 decoy-ODN treated tumor xenografts were significantly increased as compared with control groups. The positive cells were stained green under fluorescent microscope. The cumulative results showed the mean number of apoptotic cells per High Power Field (* $p < 0.05$).

STAT3 decoy-ODN inhibited proliferation and promoted apoptosis *in vivo*. Anti-Ki67 antibody, known as a human nuclear cell proliferation-associated antigen, was used as the marker for proliferation. The xenografts were prepared for paraffin sections and stained for Ki67. The Ki67 labeling index decreased by 73.2% after treatment with decoy-ODN relative to that observed in the PBS or scramble-ODN groups (Figure 3A). Furthermore, apoptotic cells were detected by TUNEL assay. As shown in Figure 3B, the number of TUNEL positive cells in STAT3 decoy-ODN treatment group was significantly greater than that in the vehicle treatment group with a ratio of 5:1 (Figure 3B). Thus, STAT3 decoy-ODN mediated the inhibitory effects on glioma growth and is involved in inhibiting proliferation and promoting apoptosis *in vivo*.

STAT3 decoy-ODN down-regulated STAT3 targeted genes at both transcription and translation levels *in vivo*. To further investigate the mechanisms of STAT3 decoy-ODN inhibitory effect on STAT3-regulated genes expression *in vivo*, xenografts were harvested and processed for RT-PCR to determine the mRNA levels of STAT3 target genes such as cell cycle control genes c-myc, cyclin D1 and cyclin E, and anti-apoptosis regulating genes bcl-2, bcl-xl and survivin. As shown in Figure 4, it was found that the mRNA levels of c-myc, cyclin D1, cyclin E, bcl-2, bcl-xl and survivin were decreased by 53.3%, 64.5%, 46.3%, 58.6%, 50.7%, and 69.5%, respectively ($p < 0.05$), while scramble-ODN had no detectable effects on them. Moreover, the tumor samples harvested from mice were immunostained for bcl-2, bcl-xl and cyclin D1. As shown in Figure 5, the intensity of the brown stain relates to the expression of target protein in tumor tissues. Microscopic examination of tumor sections demonstrated that the positive cells of cyclin D1, bcl-2 and

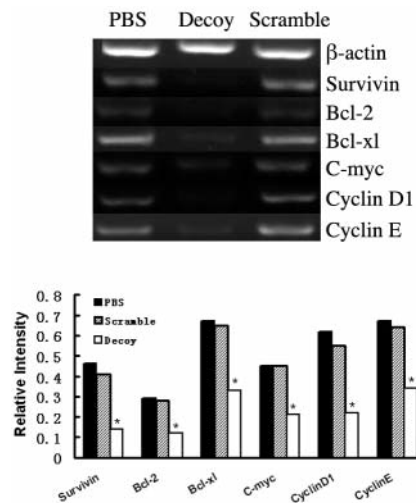


Figure 4. Blocking STAT3 down-regulated anti-apoptosis and cell cycle gene mRNA levels *in vivo*. After sacrifice, xenografts were collected and the total RNA was isolated using Trizol Reagent, mRNA levels of STAT3 targeted genes, including survivin, bcl-2, bcl-xl, cyclin D1, cyclin E and c-myc were determined using RT-PCR method. The PCR products were electrophoresed and photographed using AlphaEaseFC. Histogram presented the relative expression level of each gene after normalization to its corresponding internal control (* $p < 0.05$).

bcl-xl were decreased by 68.5%, 75.1% and 70.1%, respectively, in STAT3 decoy-ODN groups as compared with control groups. It was concluded that after blocking of STAT3 pathway by decoy-ODN, the target genes were down-regulated at both transcription and translation levels, suggesting the related genes to be involved in the inhibition of STAT3 decoy-ODN on growth of glioma *in vivo*.

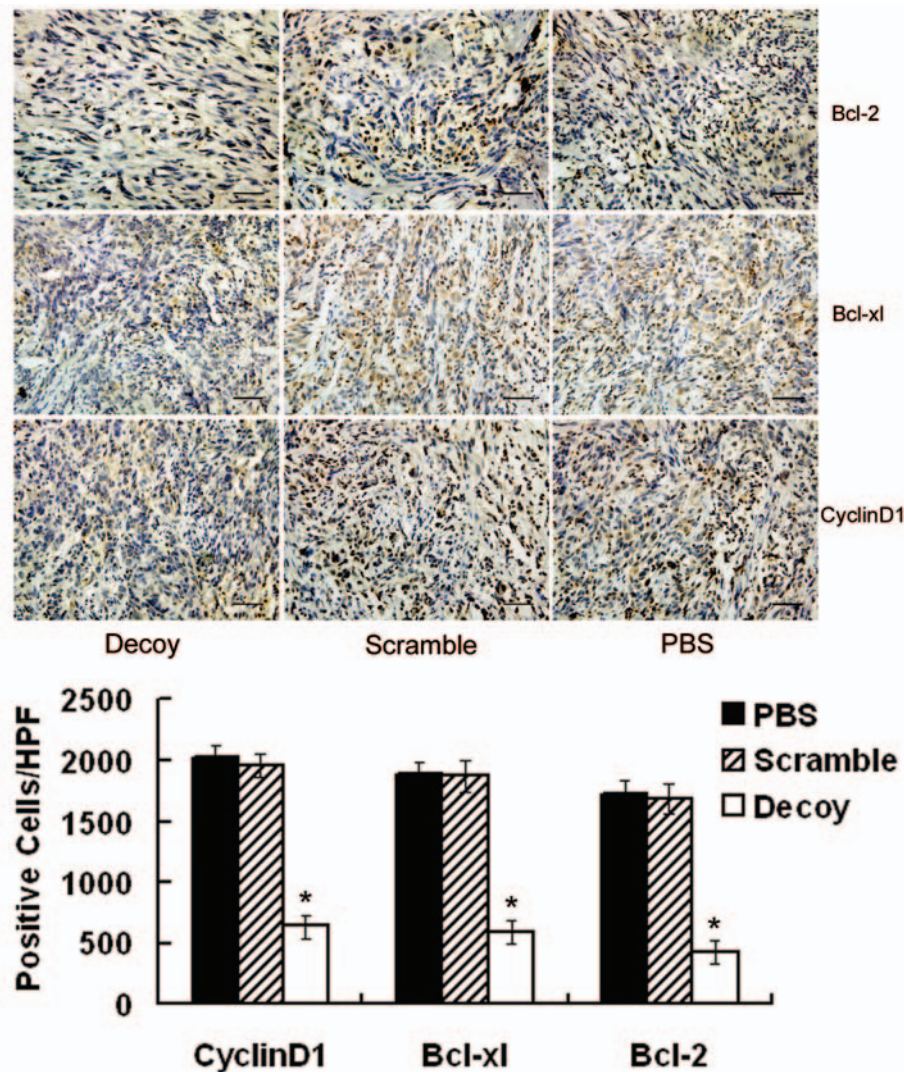


Figure 5. Blocking STAT3 down-regulated anti-apoptosis and cell cycle gene protein levels. The xenografts, harvested after mice sacrifice, were sectioned and immunohistochemical analysis performed for *bcl-2*, *bcl-xl* and *cyclin D1* as described in Materials and Methods. The staining of brown granules was in nuclei for *cyclin D1* and in cytoplasm for *bcl-2* and *bcl-xl* (SP \times 400, Black bar: 50 μ m). Values shown are the average number of *bcl-2*, *bcl-xl* or *cyclin D1* positive pixels per High Power Field in each group (* p <0.05).

Discussion

Previous studies have shown that STAT3 is constitutively activated in human gliomas and GBM cell lines (13, 18, 19), but their correlation has not been studied. This correlation was studied by Western blot using 60 frozen tissue harvested from patients suffering gliomas and U251 cell line. A strong positive correlation was observed between the persistent activation STAT3 and glioma histological grade. The phosphorylation of tyrosine-705 and serine-727 was 16.7% and 8.3% in diffuse astrocytoma, 88.9% and 27.8% in anaplastic astrocytoma and up to 100% and 100% in the glioblastoma

multiforme, respectively. In contrast, for all the 5 normal brain specimens no phosphorylation of STAT3 was observed. The data clearly demonstrated that the frequency of p-STAT3, that is, phosphorylation of tyrosine-705 or serine-727, may prompt the degree of malignance of gliomas in accordance with the diagnostic criteria of the WHO classification system (Figure 1). From diffuse astrocytoma, anaplastic astrocytoma to glioblastoma multiforme, the more malignant the gliomas were, the more activated STAT3 there was. In addition, the results showed the constitutively activated STAT3 content also varied among different primary tumor specimens in the same WHO classification. This may be due to

heterogeneity of cells or the differential turnover of STAT3 activation in tumor specimens. Therefore, these findings certified the feasibility that aberrant activated STAT3 represented a prognostic molecular marker and may be a molecular target for glioma treatment.

In a previous investigation, a double-stranded STAT3 decoy-ODN method was adopted because of its previously mentioned advantages (14, 15, 20, 21). In this earlier study, the mechanisms of inhibitory effect on the growth of U251 and A172 cell lines by blocking STAT3 *via* decoy-ODN *in vitro* were illustrated, but the condition *in vivo* was unclear. In this paper, only U251 cells were used because A172 cells could not form tumors *in vivo* according to their characteristics. Human U251 glioblastoma multiforme xenografted nude mice were used to evaluate the efficacy of STAT3 decoy-ODN *in vivo*, and the results showed that STAT3 decoy-ODN treatment significantly decreased tumor volume and tumor weight compared to PBS and scramble-ODN control (Figures 2B, 2C) in nude mice. Meanwhile, it was found that decoy-ODN led to decreased proliferation and increased apoptosis *in vivo*, as quantitated by Ki67 immunohistochemistry and TUNEL assay (Figure 3). These results demonstrated that after blocking with STAT3 decoy-ODN *in vivo*, the growth of human glioma cells could be suppressed and the apoptosis could be increased, which was consistent with the condition of human glioma cells *in vitro*.

The regulation of cell survival and cell death seems to involve death-inhibiting proteins. They are considered to play an important role in the cells apoptotic machinery. This study found that bcl-x1, bcl-2 and survivin gene expression in xenografts were down-regulated by intratumoral administration of STAT3 decoy-ODN (Figure 3), indicating that the expression of these anti-apoptotic genes is regulated by the constitutive activation of STAT3 in human glioma cells *in vivo*. Meanwhile, the protein level of bcl-x1 and bcl-2 also decreased using an immunohistochemistry assay *in vivo*. In addition, cyclin D1, c-myc and cyclin E, which are involved in cell-cycle progression arresting from G0/G1 to S phase (13) and play an important role in cell apoptosis, were also decreased in xenografts of STAT3 decoy-ODN group compared with the control groups. These data suggested that constitutively activated STAT3 contribute to tumor progression by regulating target oncogenes resisting to apoptosis and controlling tumor cell cycle progression in human glioma cells, at both transcription and translation levels.

In conclusion, a correlation between the aberrant activated STAT3 and the malignant degree of glioma has been demonstrated. The more activated STAT3, the more malignant the tumor. Further, there is a correlation between activated STAT3 in regulation of multiple genes in glioma *in*

in vivo, such as bcl-2, bcl-x1, survivin, c-myc, cyclin D1, and cyclin E. Finally, the blockade of STAT3 *via* decoy-ODN suppressed the growth of glioma cells *in vivo*, and decreased the expression of protein bcl-2, bcl-x1 and cyclin D1. Taken together with previous data, the blockade of aberrant activated STAT3 with decoy-ODN may be an efficient strategy for glioma therapy *in vivo*.

Acknowledgements

This work was supported by Natural Science Foundation of China (#30571696; #30671901; #30628014) and Ministry of Science and Technology of China (#2007AA021000; #2004CB518807)

References

- 1 Levy DE and Darnell: Stats: transcriptional control and biological impact. *Nat Rev Mol Cell Biol* 3: 651-662, 2002.
- 2 Ehret GB, Reichenbach P, Schindler U, Horvath CM, Fritz S, Nabholz M and Bucher: DNA binding specificity of different STAT proteins: Comparison of *in vitro* specificity with natural target sites. *J Biol Chem* 276: 6675-6688, 2001.
- 3 Rahaman SO, Harbor PC, Chernova O, Barnett GH, Vogelbaum MA and Haque SJ: Inhibition of constitutively active Stat3 suppresses proliferation and induces apoptosis in glioblastoma multiforme cells. *Oncogene* 21: 8403-8413, 2002.
- 4 Barton BE, Murphy TF, Shu P, Huang HF, Meyenhofen M and Barton A: Novel single-stranded oligonucleotides that inhibit signal transducer and activator of transcription 3 induce apoptosis *in vitro* and *in vivo* in prostate cancer cell lines. *Mol Cancer Ther* 3: 1183-1191, 2004.
- 5 Garcia R, Bowman TL, Niu G, Yu H, Minton S, Muro-Cacho CA, Cox CE, Falcone R, Fairclough R, Parsons S, Laudano A, Gazit A, Levitzki A, Kraker A and Jove R: Constitutive activation of Stat3 by the Src and JAK tyrosine kinases participates in growth regulation of human breast carcinoma cells. *Oncogene* 20: 2499-2513, 2001.
- 6 Alvarez JV, Grenlinch H, Sellers WR, Meyerson M and Frank DA: Signal transducer and activator of transcription 3 is required for the oncogenic effects of non-small-cell lung cancer-associated mutations of the epidermal growth factor receptor. *Cancer Res* 66: 3162-3168, 2006.
- 7 Qiu Z, Huang C, Sun J, Qiu W, Zhang J, Li H, Jiang T, Huang K and Cao J: RNA interference-mediated signal transducers and activators of transcription 3 gene silencing inhibits invasion and metastasis of human pancreatic cancer cells. *Cancer Sci* 98: 1099-1106, 2007.
- 8 Leong PL, Andrews GA, Johnson DE, Dyer KF, Xi S, Mai JC, Robbins PD, Gadiparthi S, Burke NA, Watkins SF and Rubin Grandis J: Targeted inhibition of Stat3 with a decoy oligonucleotide abrogates head and neck cancer cell growth. *PNAS* 100: 4138-4143, 2003.
- 9 Ahn JD, Morishita R, Kaneda Y, Lee SJ, Kwon KY, Choi SY, Lee KU, Park JY, Moon IJ, Park JG, Yoshizumi M, Ouchi Y and Lee IK: Inhibitory effects of novel AP-1 decoy oligodeoxynucleotides on Vascular Smooth Muscle Cell proliferation *in vitro* and neointimal formation *in vivo*. *Circulation Research* 90: 1325-1332, 2002.

- 10 Crinelli R, Bianchi M, Gentilini L and Magnani M: Design and characterization of decoy oligonucleotides containing locked nucleic acids. *Nucleic Acids Res* 30: 2435-2443, 2002.
- 11 Morishita R, Tomita N, Kaneda Y and Ogihara T: Molecular therapy to inhibit NF-KB activation by transcription factor decoy oligonucleotides. *Current Opinion in Pharmacology* 4: 139-146, 2004.
- 12 Tomita T, Kunugiza Y, Tomita N, Takano H, Morishita R, Kaneda Y and Yoshikawa H: E2F decoy oligodeoxynucleotide ameliorates cartilage invasion by infiltrating synovium derived from rheumatoid arthritis. *Int J Mol Med* 18: 257-65, 2006.
- 13 Gu JH, Li G, Sun T, Su YH, Zhang XL, Shen J, Tian ZG and Zhang J: Blockage of STAT3 signaling pathway with a decoy oligonucleotide suppresses growth of human malignant glioma cells. *J Neurooncol* 89: 9-17, 2008.
- 14 Sun X, Zhang J, Wang L and Tian Z: Growth inhibition of human hepatocellular carcinoma cells by blocking STAT3 activation with decoy-ODN. *Cancer Lett* 262: 201-213, 2008.
- 15 Zhang X, Zhang J, Wang L, Wei H and Tian Z: Therapeutic effects of STAT3 decoy oligodeoxynucleotide on human lung cancer in xenograft mice. *BMC Cancer* 7: 149, 2007.
- 16 Xi S, Gooding WE and Rubin Grandis J: *In vivo* antitumor efficacy of STAT3 blockade using a transcription factor decoy approach: implications for cancer therapy. *Oncogene* 24: 970-979, 2005.
- 17 Morishita R, Tomita N, Kaneda Y and Ogihara T: Molecular therapy to inhibit NFkappaB activation by transcription factor decoy oligonucleotides. *Curr Opin Pharmacol* 4: 139-146, 2004.
- 18 Schaefer LK, Ren Z, Fuller GN and Schaefer TS: Constitutive activation of Stat3alpha in brain tumors: localization to tumor endothelial cells and activation by the endothelial tyrosine kinase receptor (VEGFR-2). *Oncogene* 21: 2058-2065, 2002.
- 19 Konnikova L, Kotecki M, Kruger MM and Cochran BH: Knockdown of STAT3 expression by RNAi induces apoptosis in astrocytoma cells. *BMC Cancer* 3: 150, 2003.
- 20 Shimizu H, Nakagami H, Tsukamoto I, Morita S, Kunugiza Y, Tomita T, Yoshikawa H, Kaneda Y, Ogihara T and Morishita R: NFkappaB decoy oligodeoxynucleotides ameliorates osteoporosis through inhibition of activation and differentiation of osteoclasts. *Gene Ther* 13: 933-941, 2006.
- 21 Yamasaki K, Asai T, Shimizu M, Aoki M, Hashiya N, Sakonjo H, Makino H, Kaneda Y, Ogihara T and Morishita R: Inhibition of NFkappaB activation using cis-element 'decoy' of NFkappaB binding site reduces neointimal formation in porcine balloon-injured coronary artery model. *Gene Ther* 10: 356-364, 2003.

Received October 27, 2008

Revised January 5, 2009

Accepted January 27, 2009